Electronic Supporting Information (ESI) for:

Improved thermoset materials derived from biobased terpene macromolecules via photo-crosslinking

Dimitrios Skoulas,[a] Fernando Bravo[a] and Arjan W. Kleij[a,b]*

[a] Institute of Chemical Research of Catalonia (ICIQ-CERCA), Barcelona Institute of Science & Technology (BIST), Av. Països Catalans 16, 43007 – Tarragona (Spain). E-mail: akleij@iciq.es

[b] Catalan Institute of Research and Advanced Studies (ICREA), Pg. Lluís Companys 23, 08010 – Barcelona (Spain)

Table of Contents:

S3. Materials

PLC was prepared according to the literature guidelines.[1] Ethane-1,2-dithiol, 1,7-octadiene, limonene, geraniol and divinylbenzene (DVB) were purchased from Merck. Phenyl-bis(2,4,6-trimethylbenzoyl) phosphine oxide (BAPO) was purchased from TCI.

S3. Methods

IR spectra were recorded on a Bruker Tensor 27 FT-IR spectrometer. Characteristic absorption wave numbers are reported in cm^{-1}. Differential scanning calorimetry (DSC) analyses were measured under a N_2 atmosphere using a Mettler Toledo equipment (model DSC822e). Samples were weighed into 40 μL aluminium crucibles and subjected to three heating cycles at a heating rate of 10 °C/min. Thermogravimetric analyses (TGA) were recorded under N_2 atmosphere using Mettler Toledo equipment (model TGA/SDTA851). Samples were weighed into 40 μL aluminium crucibles and heated to 600 ºC at a heating rate of 10 °C/min. Gel permeation chromatography (GPC) measurements were performed using an Agilent 1200 series HPLC system, equipped with PSS SDV Analytical linear M GPC column (8 × 300 mm; 5 μm particle size) in tetrahydrofuran at 30 °C at a flow rate of 1 mL·min^{-1}. Samples were analyzed at a concentration of 1 mg·mL^{-1} after filtration through a 0.45 μm pore-size membrane. M_n, M_w, and $Đ$ data were derived from the RI signal by a calibration curve based on polystyrene standards (PS from Polymer Standards Service) for the analysis of the polymers. The GPC samples were prepared by dissolving the polymer (2 mg) in THF (2 mL), and filtering the solution through a 0.45 μm pore-size membrane. Polymer density was determined by helium pycnometry measurements carried out on a Quantachrome micro Ultrapyc 1200e. Samples were purged for 5 min before the measurement. The system was set up to collect 5 runs, and the values reported are the average of the last 3 samples, provided the standard deviation fulfills the criteria of being <5%.

S3. Dynamic Mechanical Properties

The determination of the dynamic mechanical properties of the different samples supplied have been done according to the following standards:

> ISO 6721-1:2011 "Plastics -- Determination of dynamic mechanical properties -- Part 1: General principles".

> ISO 6721-4:2019 "Plastics — Determination of dynamic mechanical properties — Part 4: Tensile vibration — Non-resonance method"

> ISO 6721-11: 2012 "Plastics -- Determination of dynamic mechanical properties -- Part 11: Glass transition temperature".

The first standard specifies methods for determining the dynamic mechanical properties of rigid plastics within the region of linear viscoelastic behaviour. The second one is the description of the specific test method for the tensile test. The last part of the ISO 6721 (part

11) specifies methods for determining a value of the glass transition temperature (T_g) from the dynamic mechanical properties measured during a linear temperature scan under heating conditions.

According to these standards, a tensile vibration method was used to determine the components of Young's complex modulus (storage modulus, loss modulus, and tan delta) of the sample at a specific frequency as a function of temperature. From these data, a value for the glass transition was determined.

S4. CONDITIONS:

Dynamic Mechanical Analyser DMAQ850 from TA Instrument.
Mode of Deformation: tensile
Frequency 1 Hz.
Oscillation strain imposed 0.0075% (calculated to be within the linear viscoelastic range).
Static Force 0.01 N
Heating/cooling rate: 2 ºC/min.
Temperature Range: -50 ºC to 120/150 ºC
Clamp/Mode deformation: dual screw film clamp.

S5. BENDING ANALYSES

TESTING PROCEDURE:

The determination of the bending analysis of the different samples has been done according to the following procedure: A rectangular sample of the material tested was placed in the DMA apparatus (testing in static mode, rate control strain ramp) at room temperature and tested in 3-point bending. An increasing centred force was applied with a strain rate of 0.1 mm/min. The Force and displacement were registered and the corresponding stress and strain values were calculated using classical Euler-Bernoulli Beam Theory and, thus, the Bending Modulus.

CONDITIONS:

Dynamic Mechanical Analyser DMAQ850 from TA Instrument.
Static mode, rate control strain ramp
Mode of Deformation: 3-point bending
Span: 10 mm
Static Force 0.01 N
Temperature: 28°C
Clamp/Mode deformation: 3-point bending low friction.

S6. TENSILE ANALYSES

TESTING PROCEDURES:

The determination of the tensile properties of the different samples supplied have been done according to the following standards: ISO 527-1: 2020. "Plastics. Determination of tensile properties General principles" ISO 527-2:2012 "·Plastics - Determination of tensile properties - Part 2: Test conditions for moulding and extrusion plastics". This tensile test is used to determine essential mechanical properties of moulding materials. These characteristic values are mostly used for comparison purposes. The standards ISO 527-1 (general principles) and ISO 527-2 (test conditions for moulding and extrusion materials) describe tensile testing on plastics. The guiding principle of the ISO 527 standard is the high reproducibility of test results across laboratories, companies and national borders. These standards stablish the methods used to investigate the tensile behaviour of the test specimens and for determining the tensile strength, tensile modulus and other aspects of the tensile stress/strain relationship under the conditions defined.

TESTING CONDITIONS:

Tensile Testing Machine: Shimadzu AGS-X
Load Cell: 1 kN
Mode of Deformation: tensile
Speed: 5 mm/min
Temperature: 25 °C (± 2 °C)

RESULTS:

Stress is computed as the force dived by the initial cross section (width × thickness) and the strain is computed as the displacement of the crosshead divided by the initial distance between grips. The Tensile Modulus (in MPa) is computed as the slope of the linear part of each stress-strain curve. The Energy Absorbed at break (in kJ/m^3) is calculated as the area below the stress-strain curve.

S7. SEM analyses

Scanning electron microscopy (SEM) was performed on an Analytic FEI Quanta FEG 200 microscope (FEI, Hillsboro, OR, USA) with an acceleration voltage of 10-20 kV. Note that these SEM analysis data was obtained at the University Rovira i Virgili in Tarragona (URV, Spain).
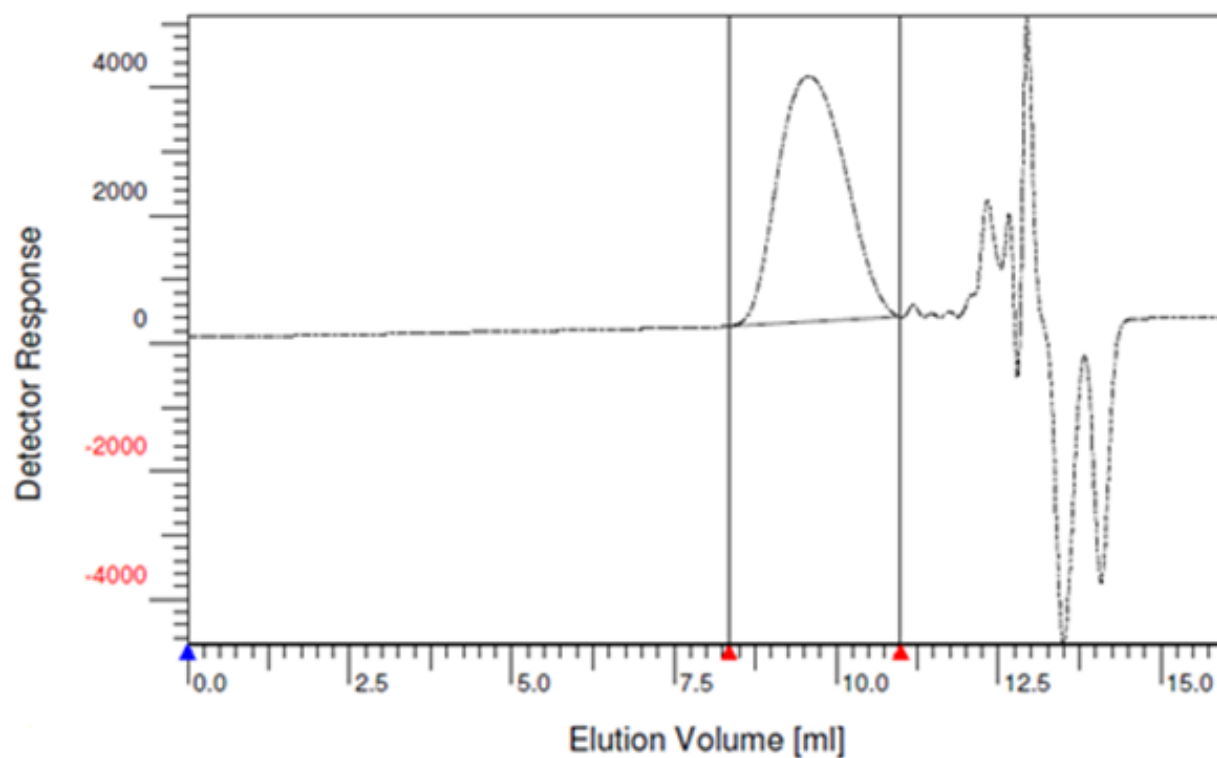
S8. PLC Characterization

Figure S1: GPC chromatogram of the PLC used.

Table S1: Molecular Characteristics of PLC obtained by GPC analysis.

M_n (g/mol)	M_w (g/mol)	M_z (g/mol)	Đ
7.5666e3	1.0661e4	1.4536e4	1.4090e0
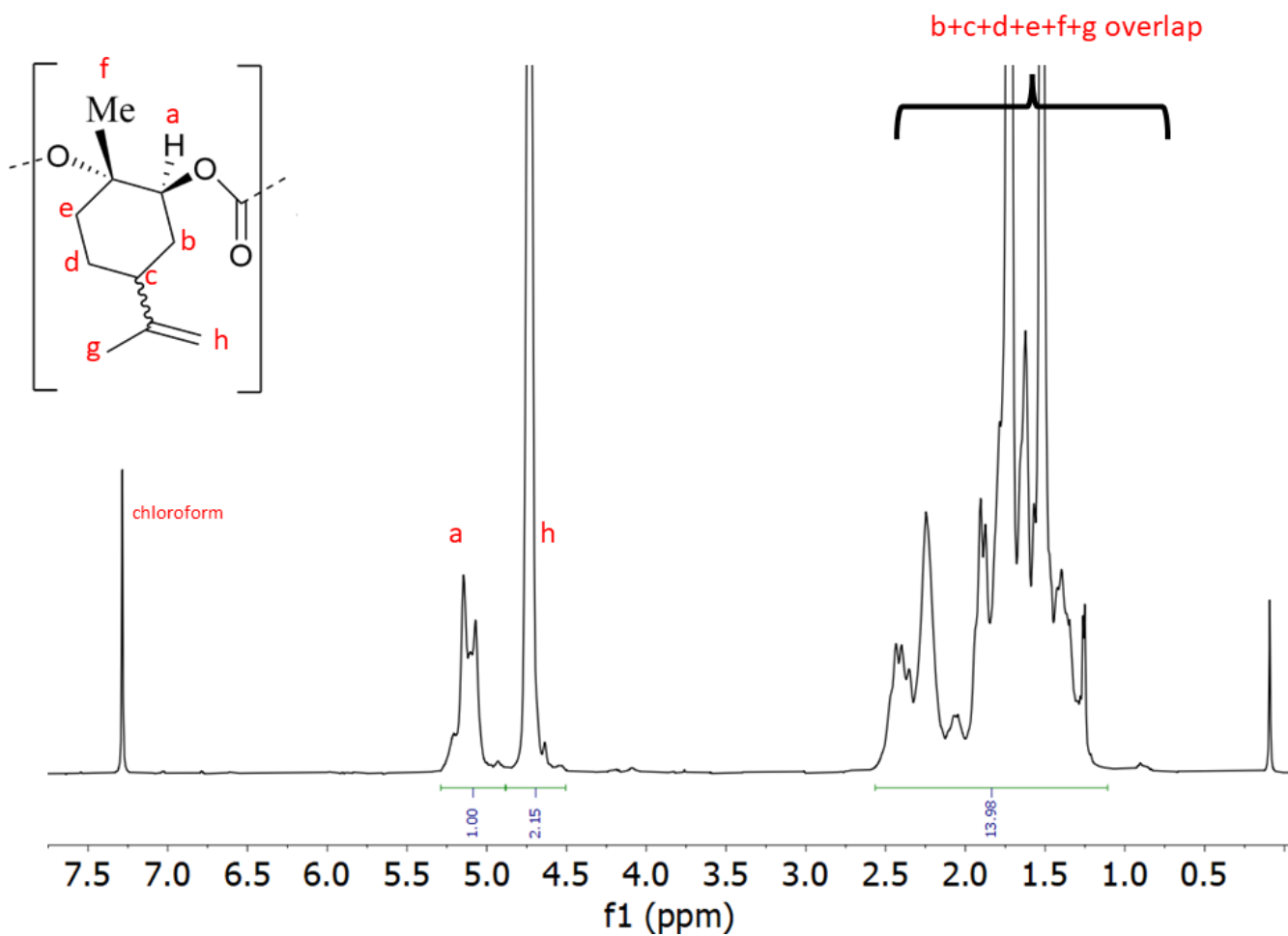
Figure S2: ^1H NMR (CDCl$_3$, 400 MHz) spectrum of PLC.

S10. IR Analyses
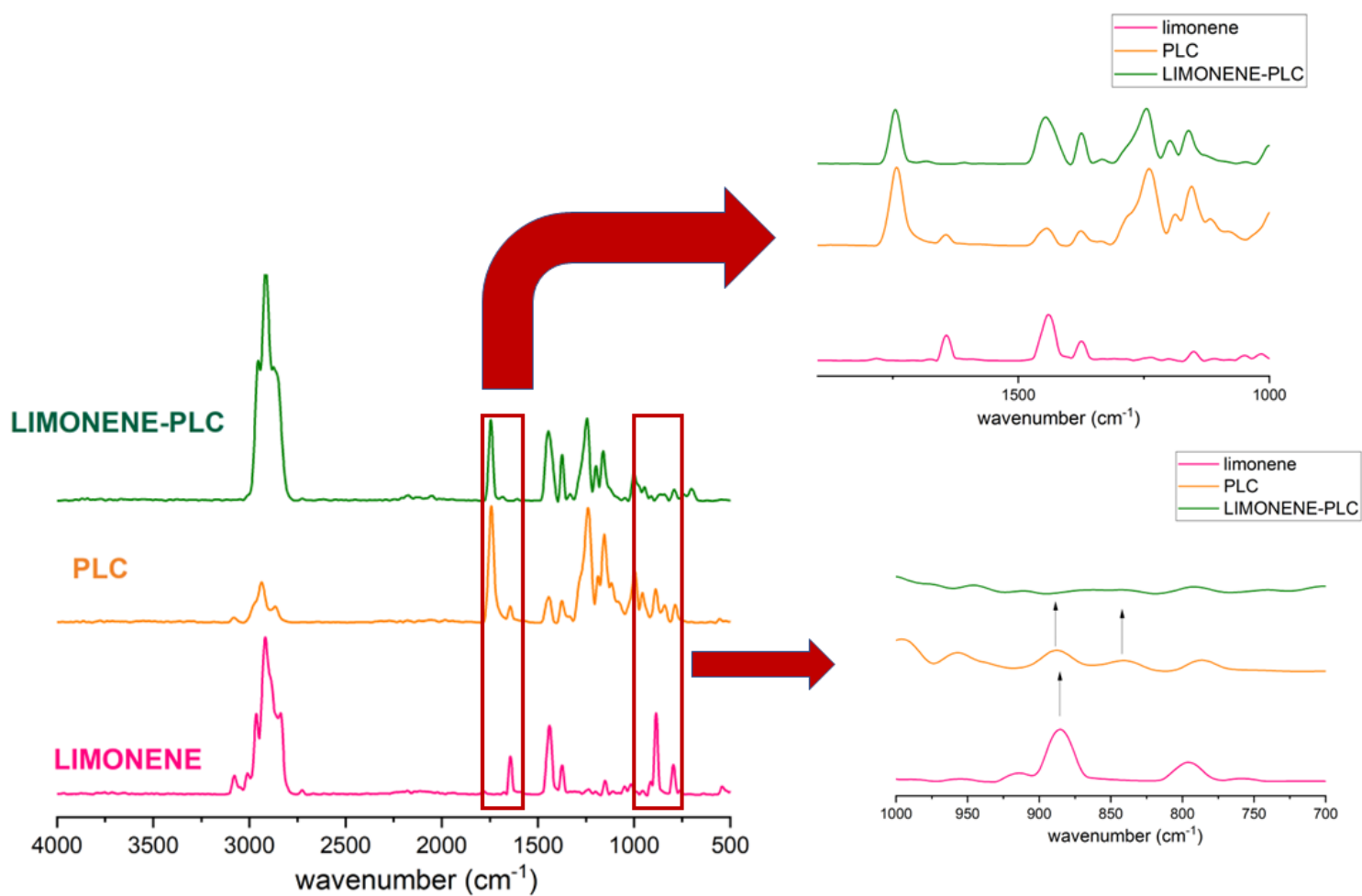
*Figure S3: IR spectrum analysis of **M5**, PLC and limonene.*
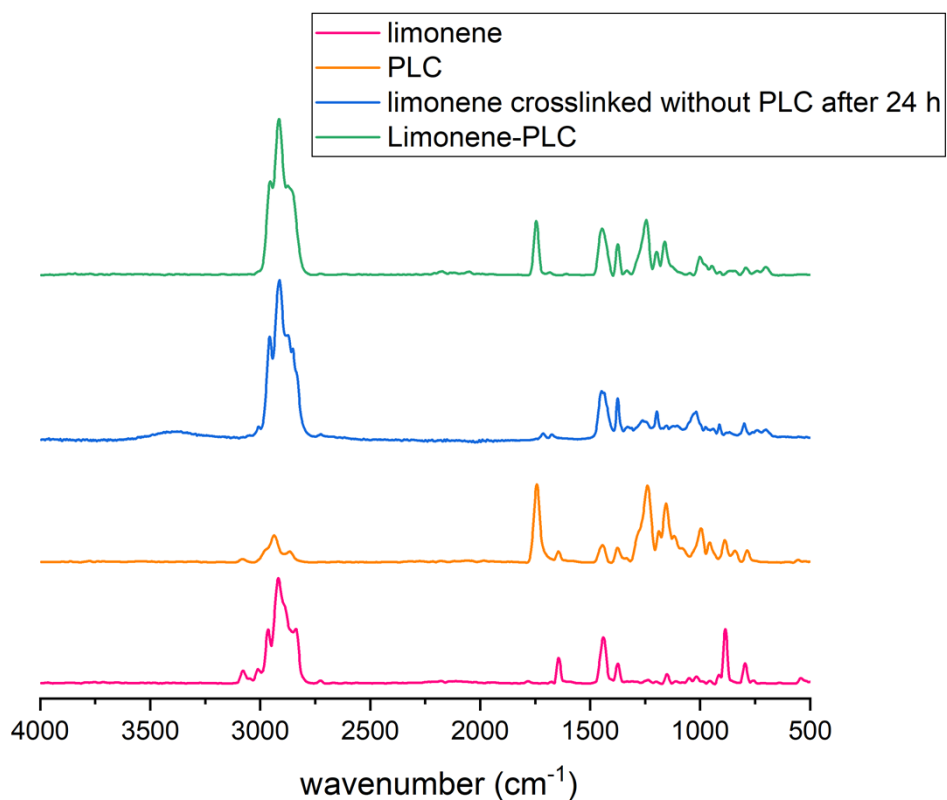
Figure S4: IR spectrum analysis of Limonene, Limonene-PLC after 20 minutes of irradiation, PLC and Limonene crosslinked without PLC after 24 h. After 20 minutes no difference was observed for limonene crosslinked without PLC.
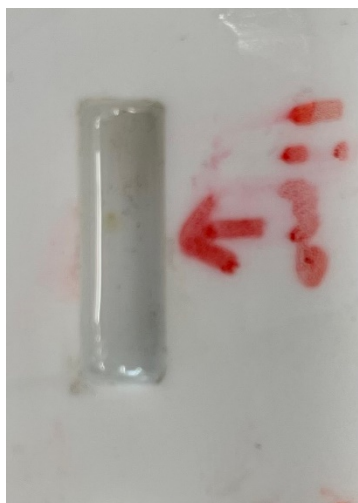
Figure S5: Photo of Limonene crosslinked without PLC after 24 h.
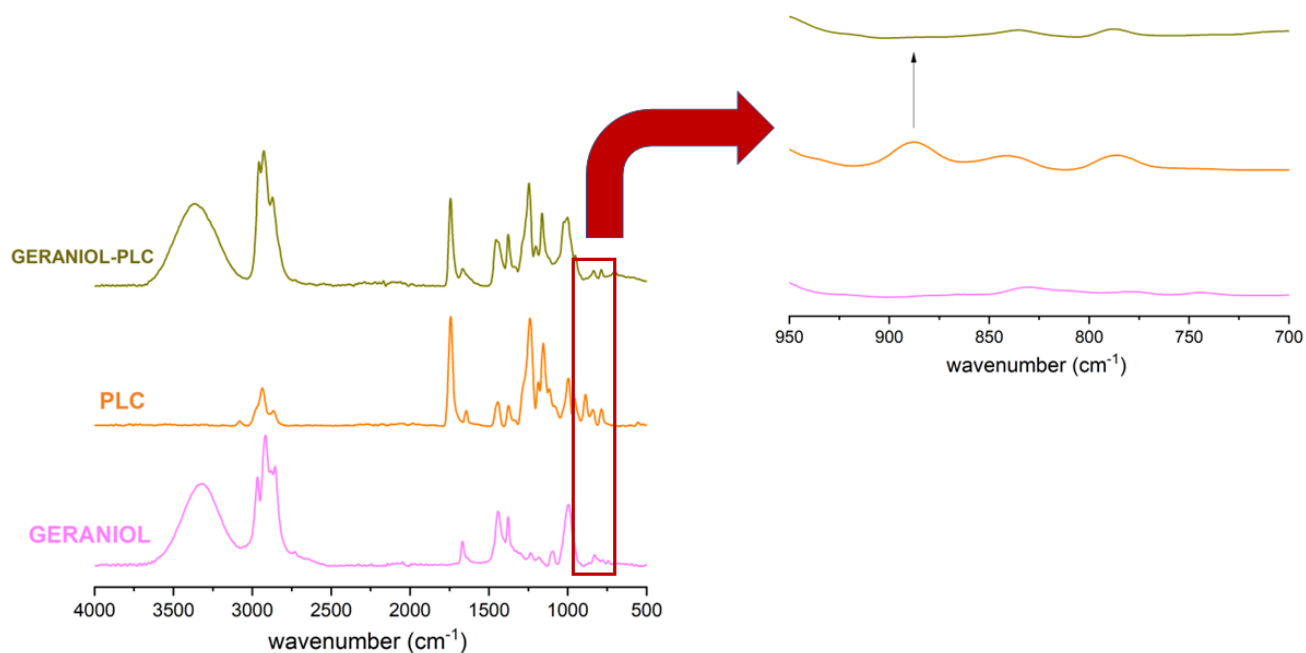
*Figure S6: IR spectrum analysis of **M6**, PLC and geraniol.*
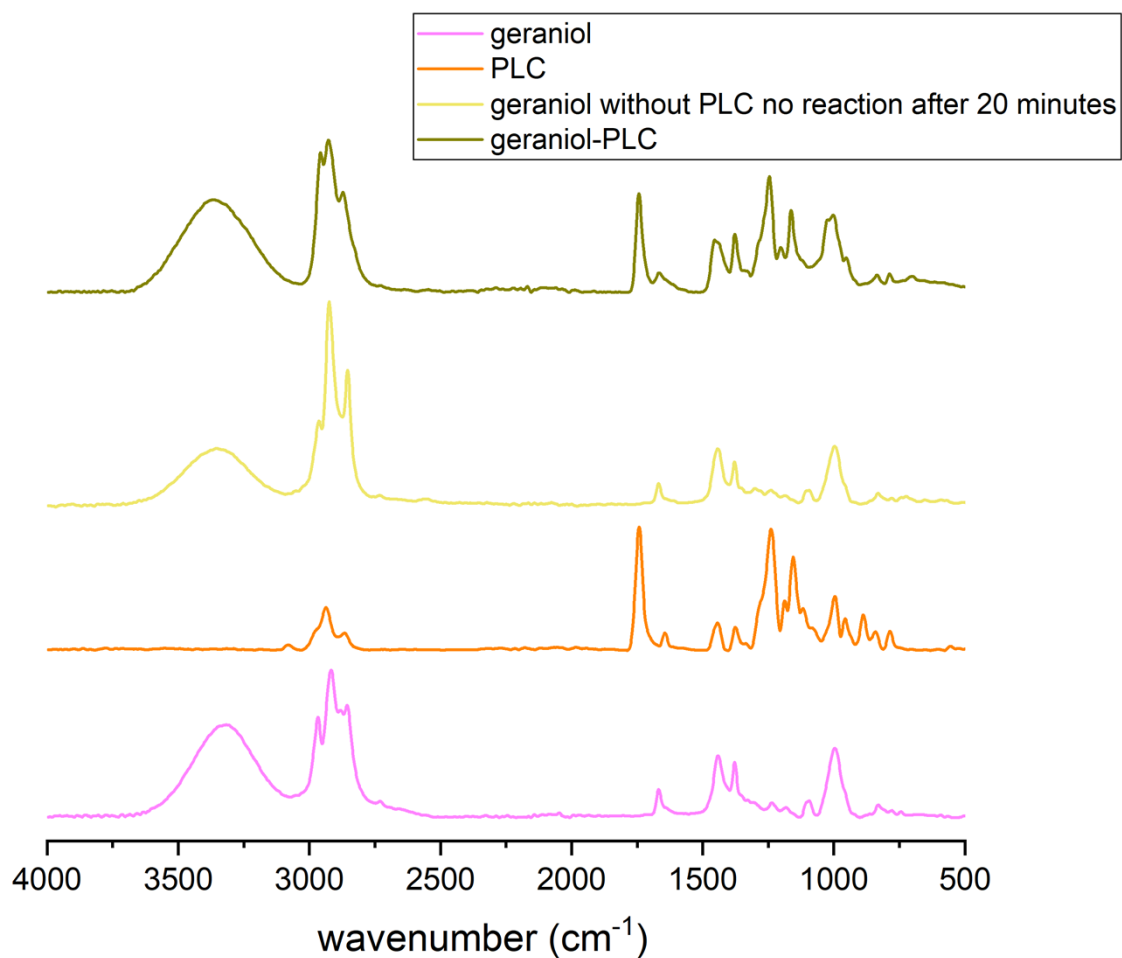
*Figure S7: IR spectrum analysis of **M6** (after 20 minutes of irradiation), PLC, geraniol and geraniol crosslinked without PLC after 20 minutes of irradiation.*

Figure S8: Photo of Geraniol crosslinked without PLC after 20 minutes.

Figure S9: Molds used for the preparation of the DMA samples.

S14. Results of Dynamic Mechanical Analyses
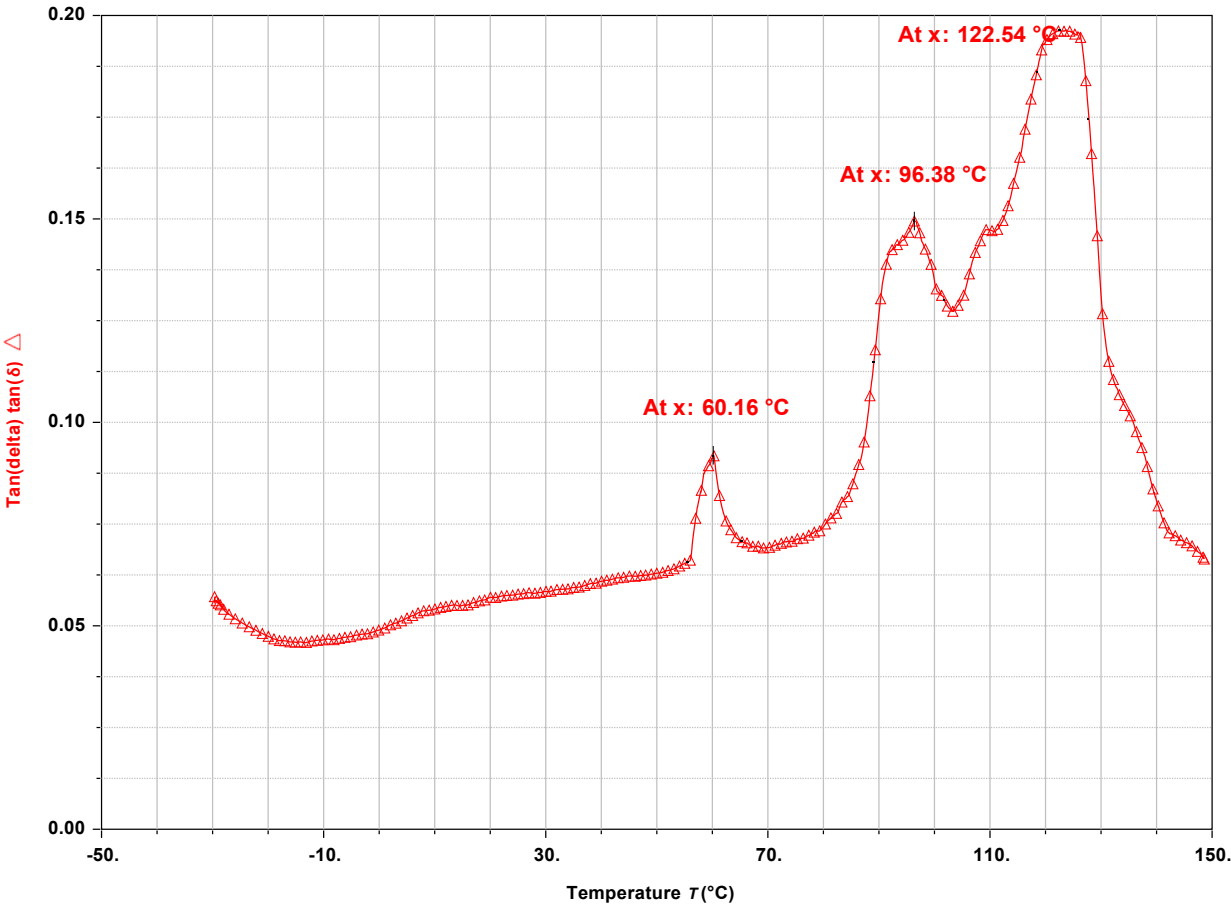
*Figure S10: Analysis of tan-δ of **M1***
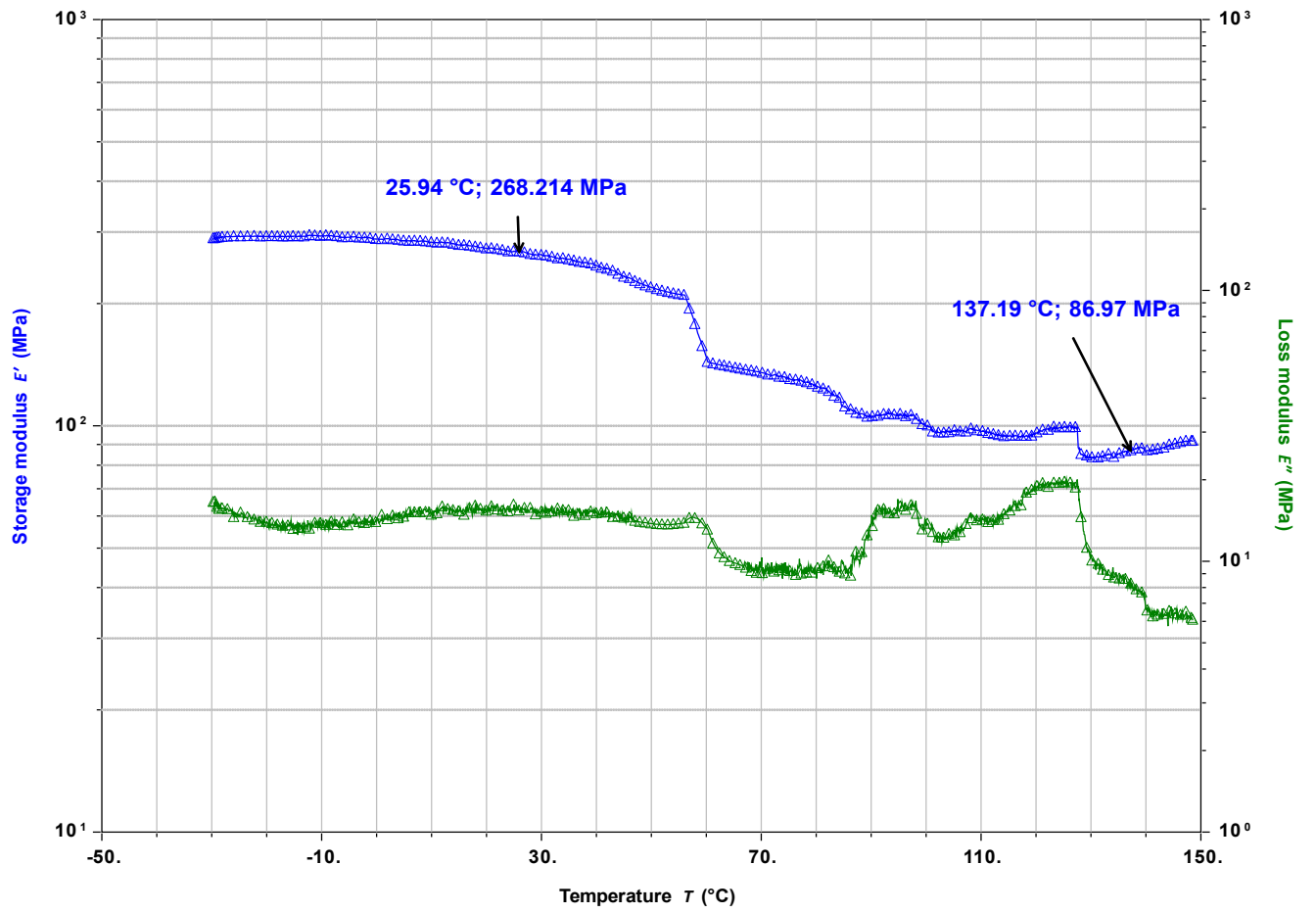
*Figure S11: Analysis of Complex Modulus of **M1**.*
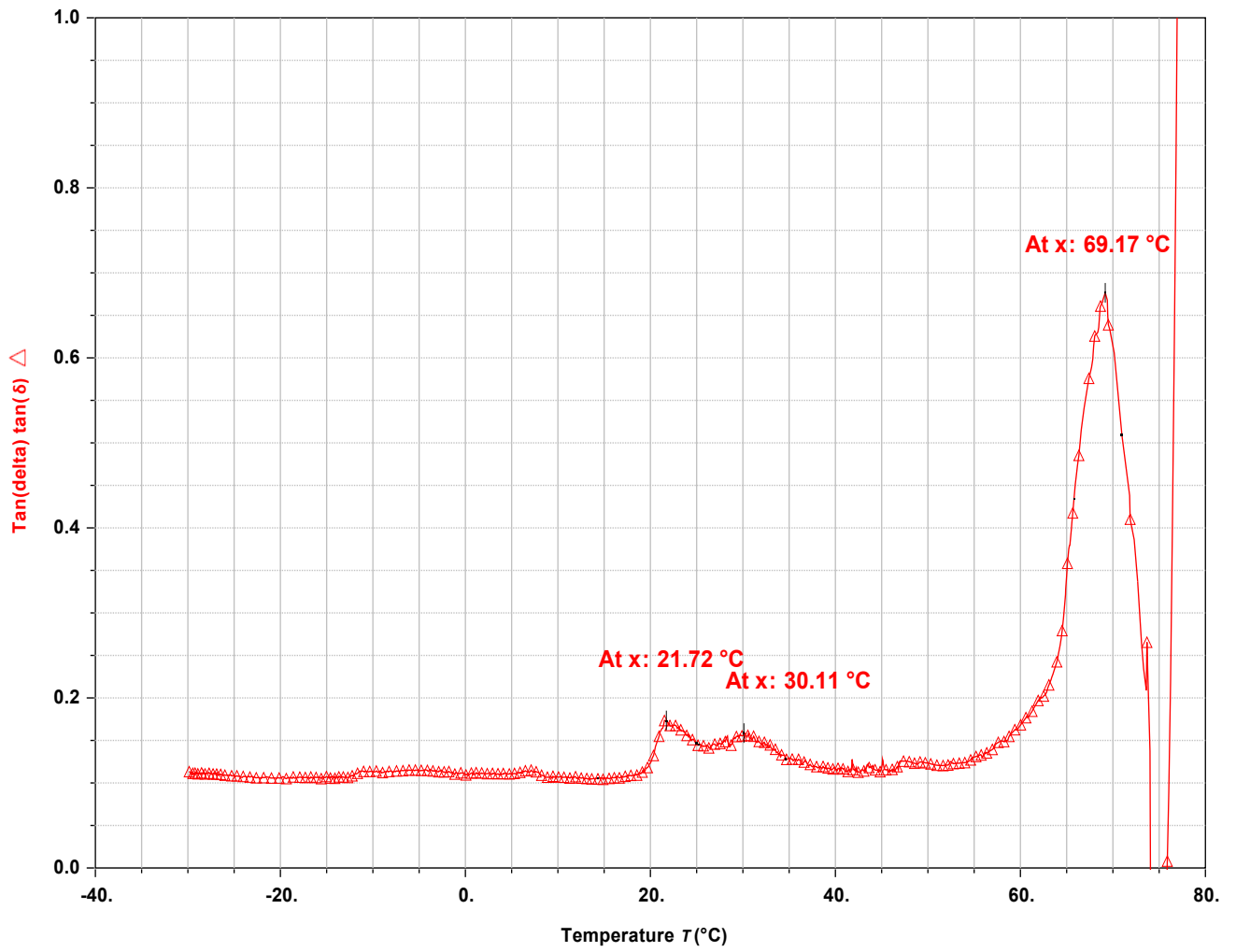
*Figure S12: Analysis of tan-δ of **M2***
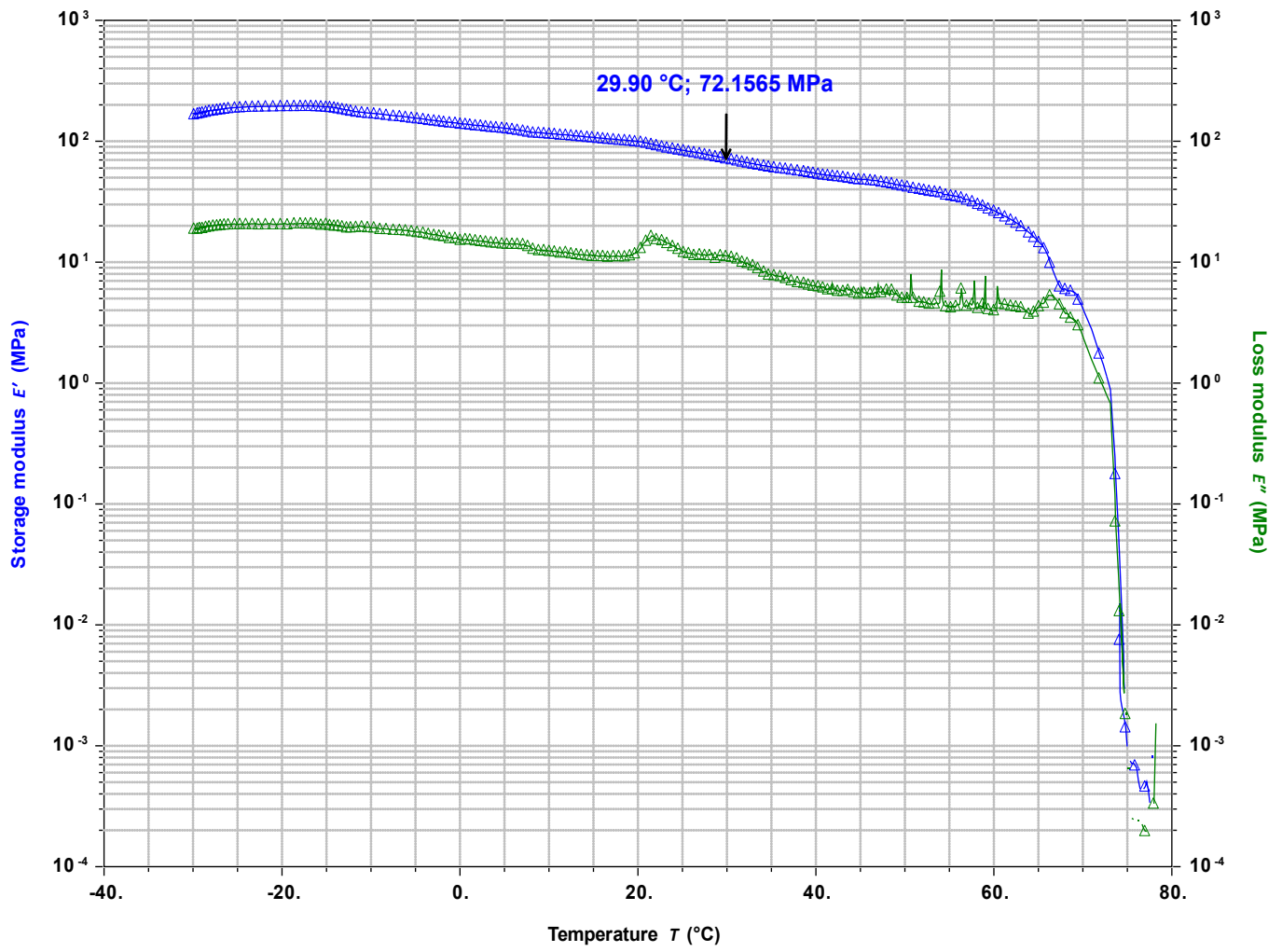
Figure S13: Analysis of Complex Modulus of **M2**
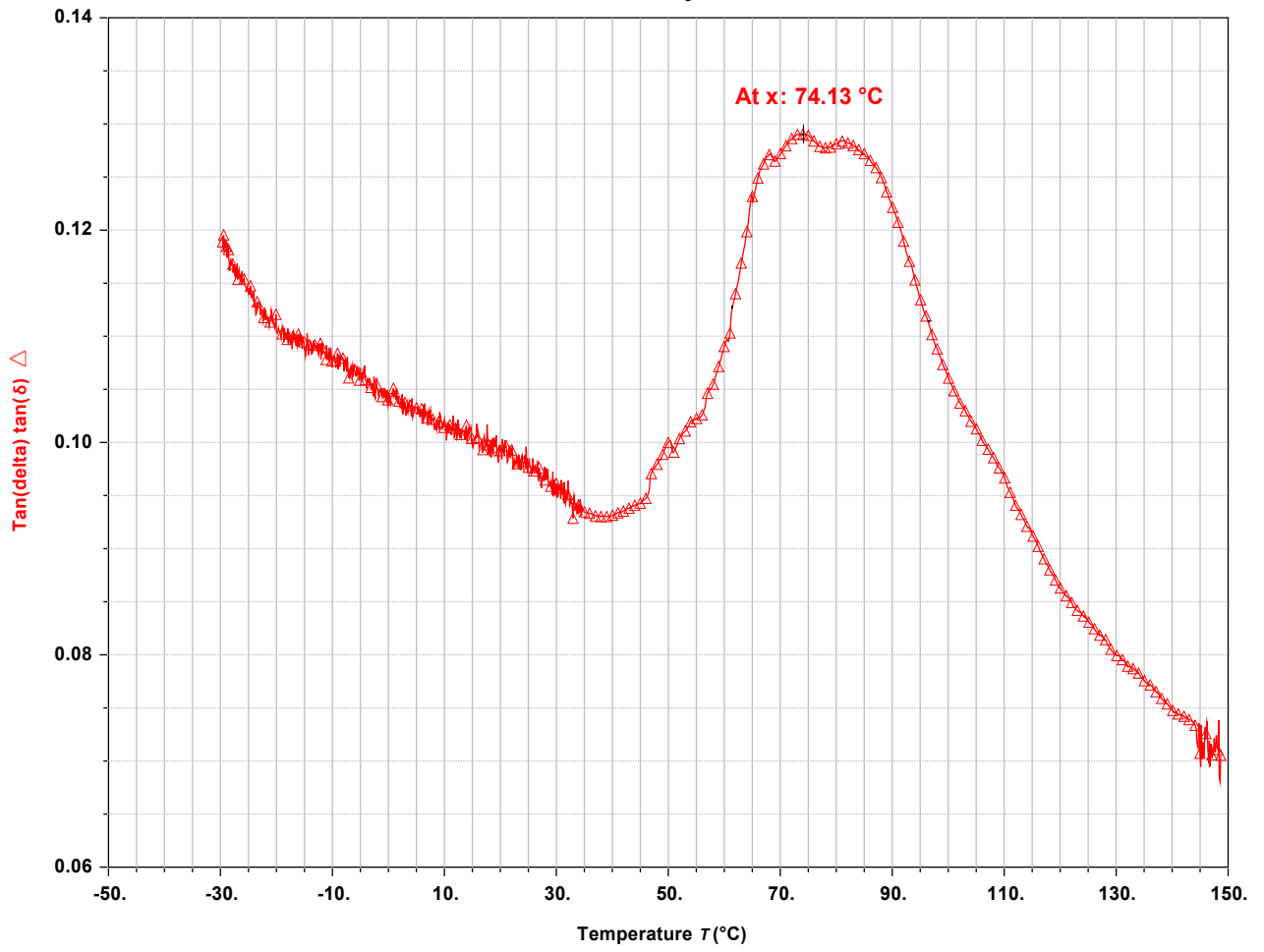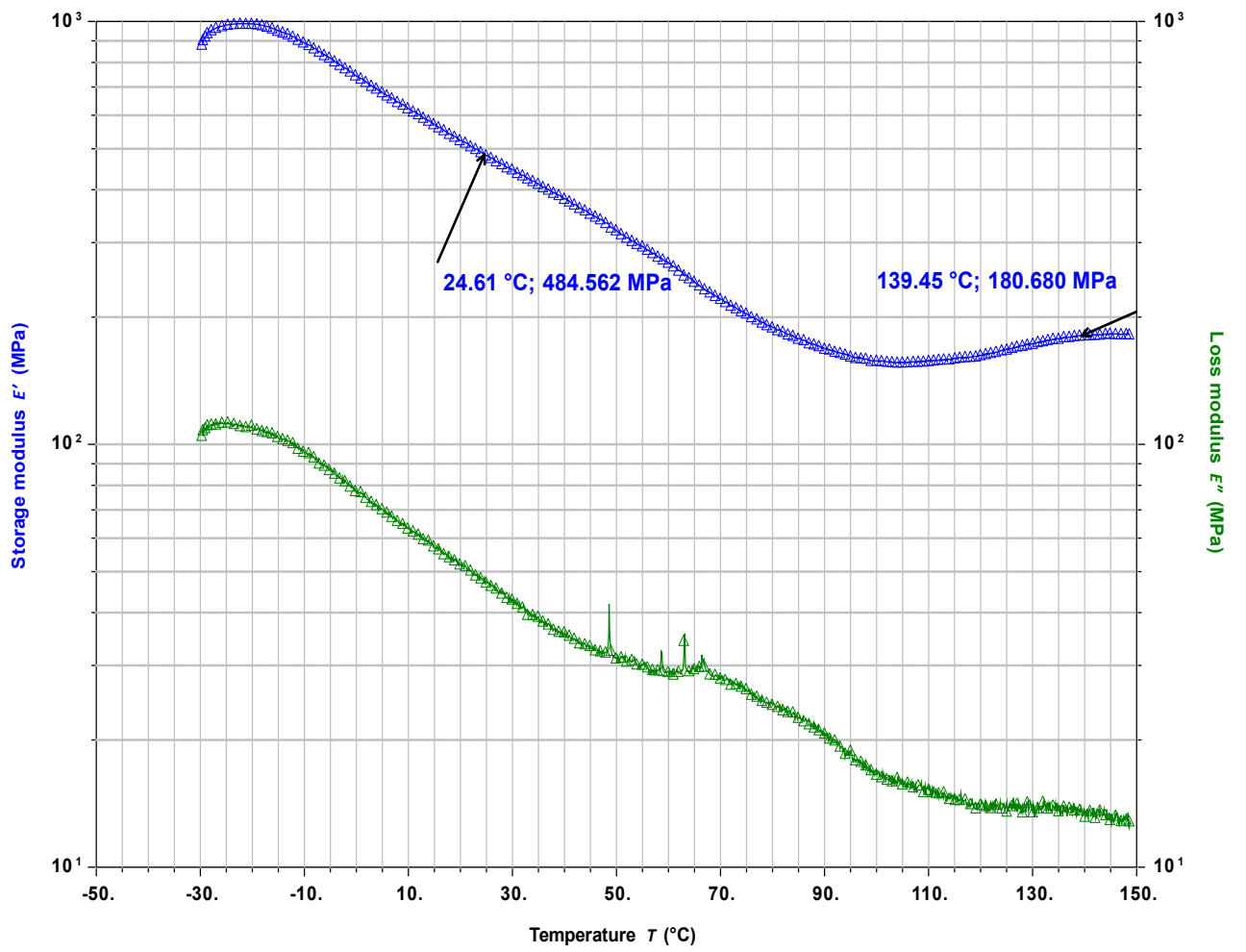
*Figure S14: Analysis of tan-δ of **M3**.*
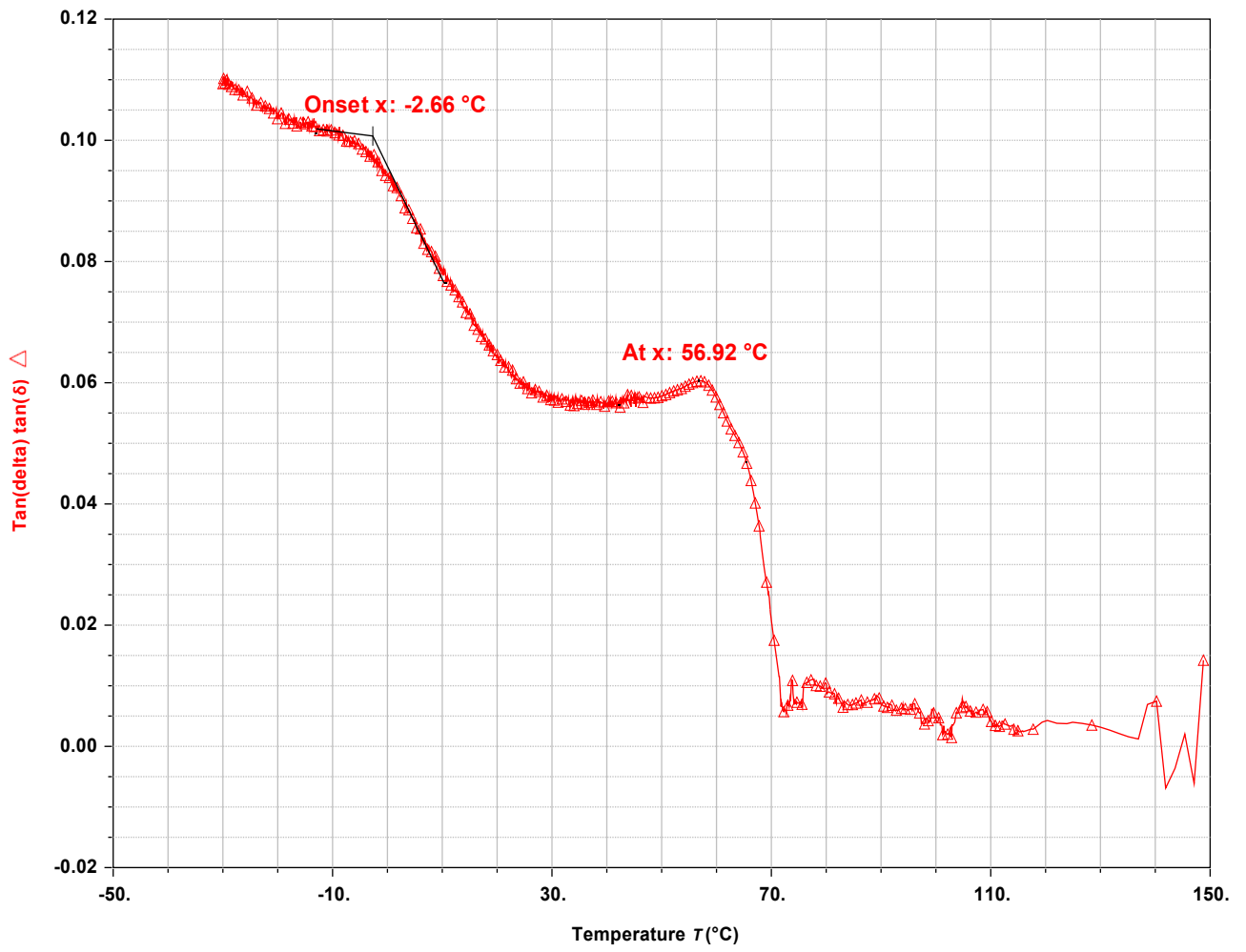
*Figure S15: Analysis of Complex Modulus of **M3***
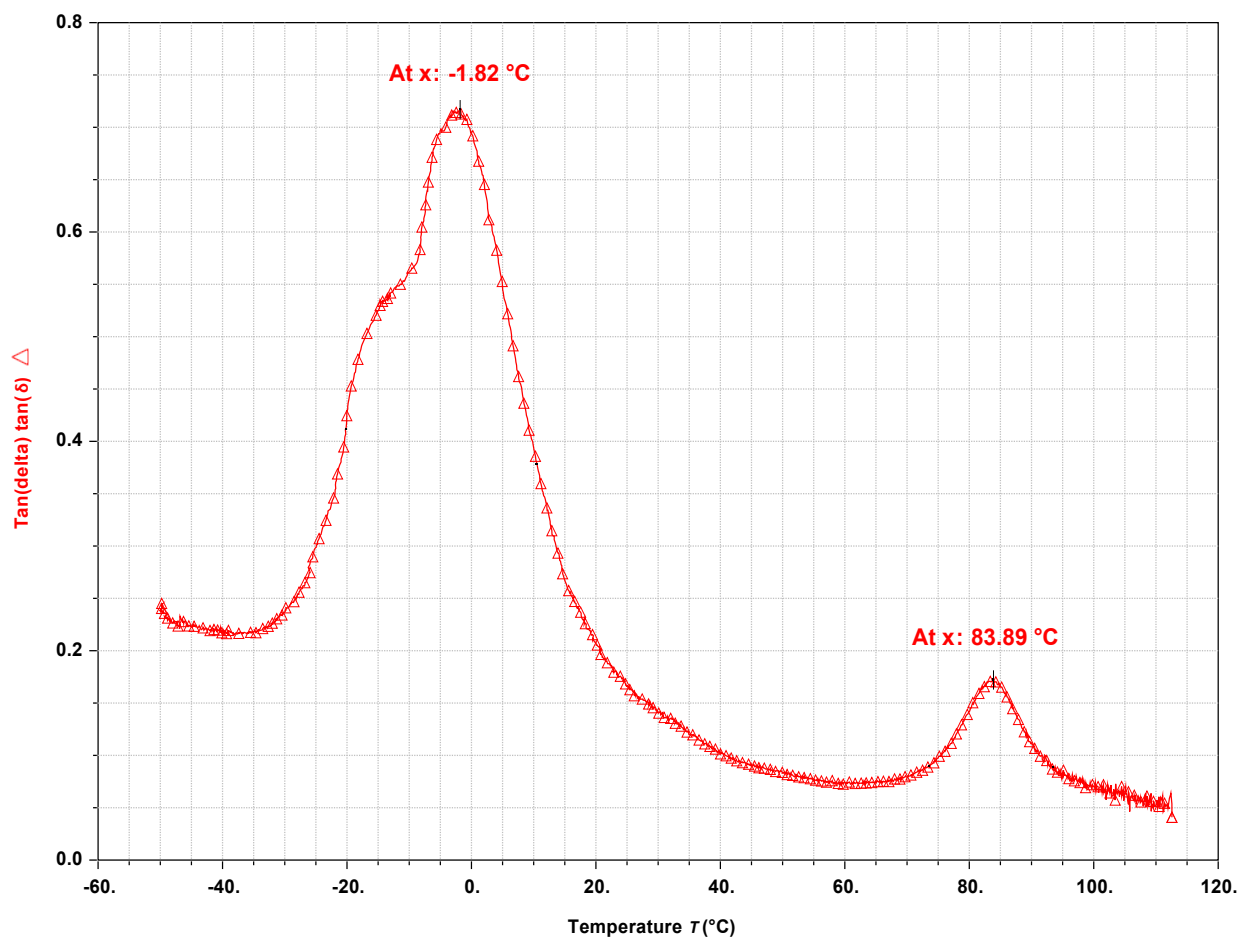
*Figure S16: Analysis of tan-δ of **M4***
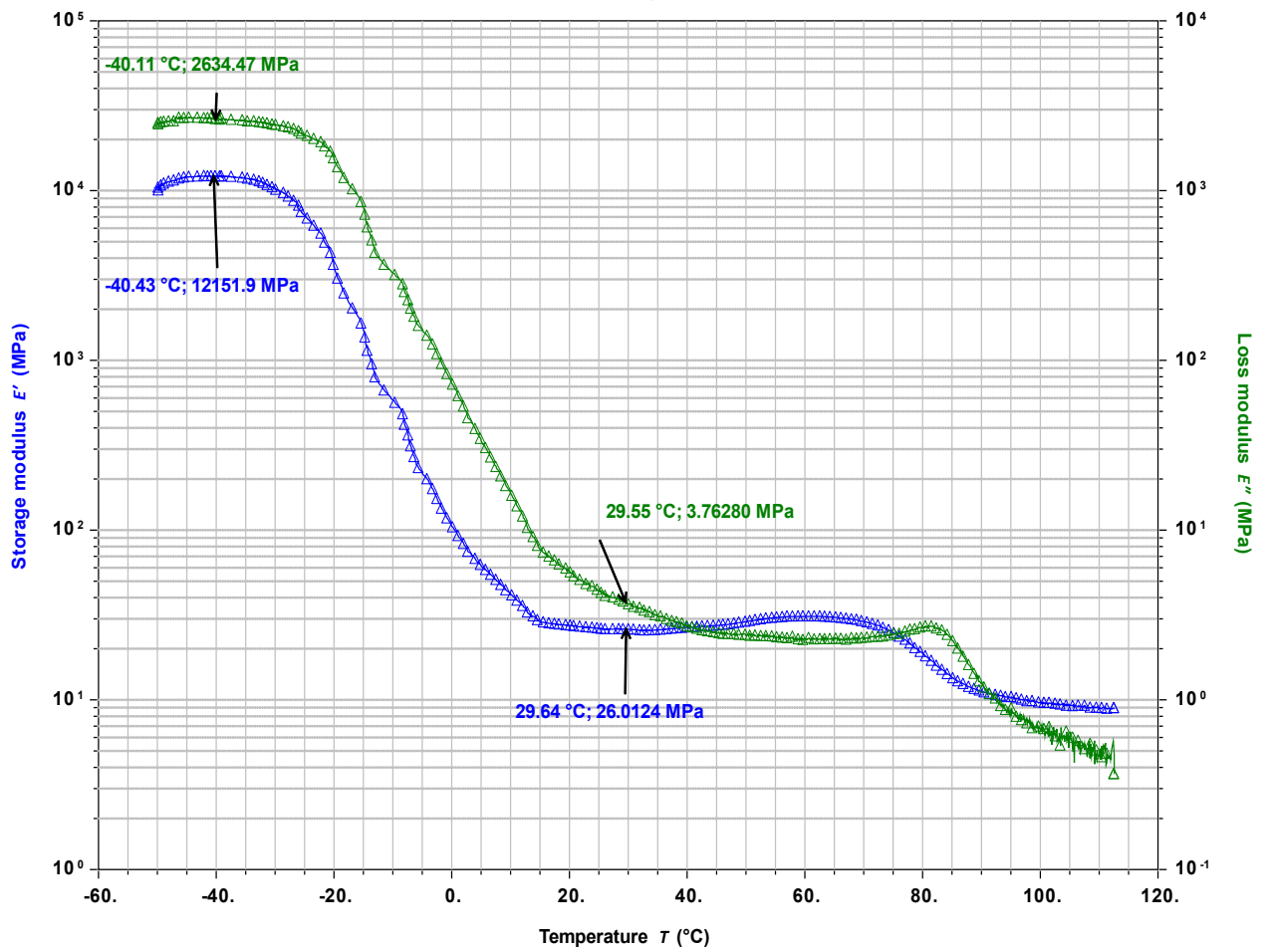
*Figure S17: Analysis of tan-δ of **M5***
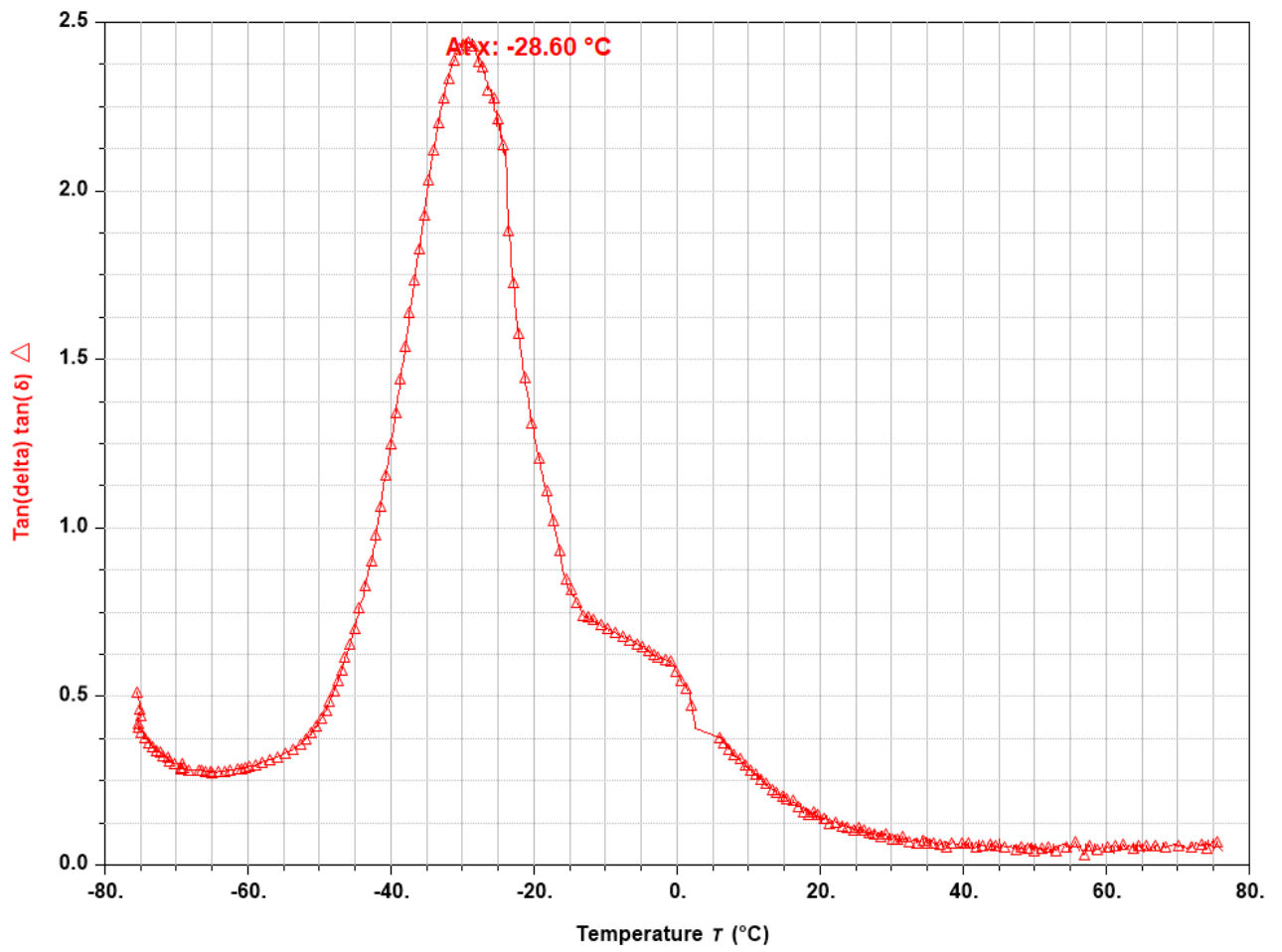
*Figure S18: Analysis of Complex Modulus of **M5***
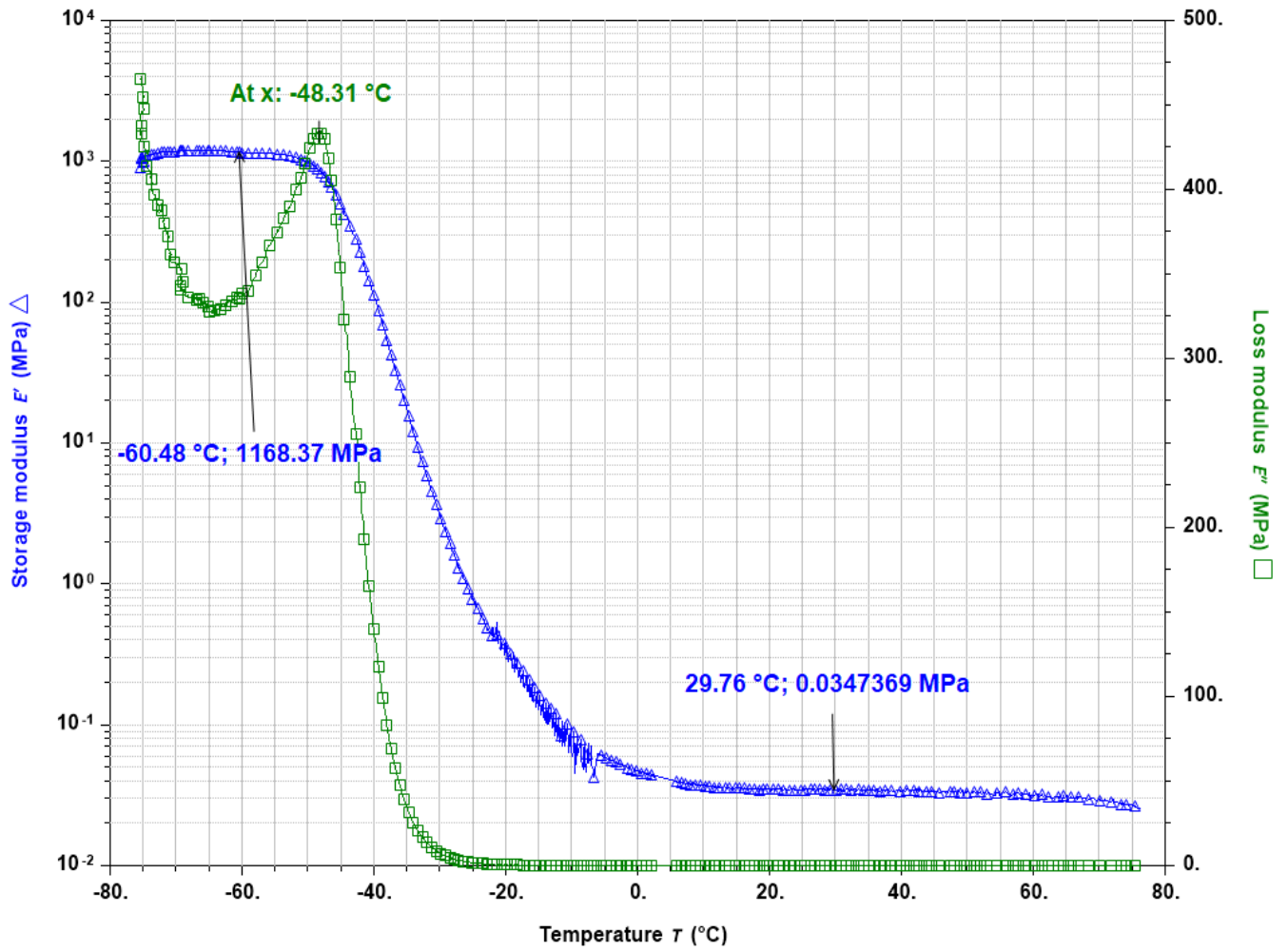
*Figure S19: Analysis of tan-δ of **M6***

*Figure S20: Analysis of Complex Modulus of **M6***
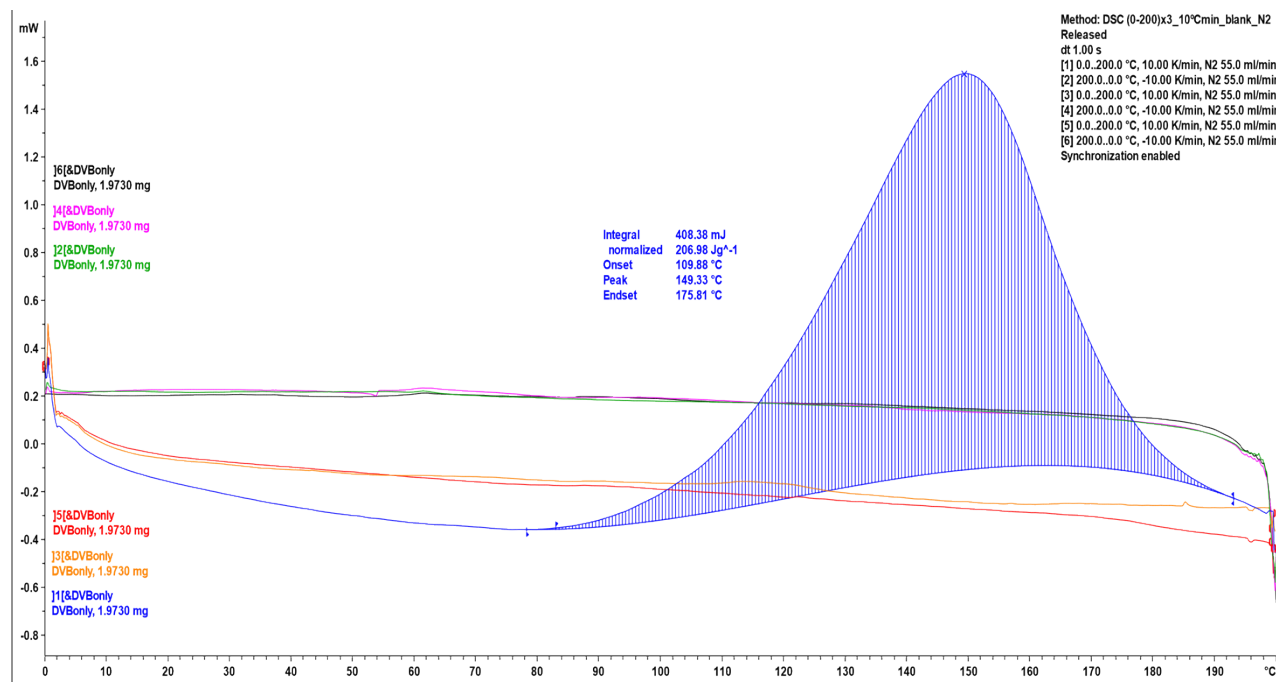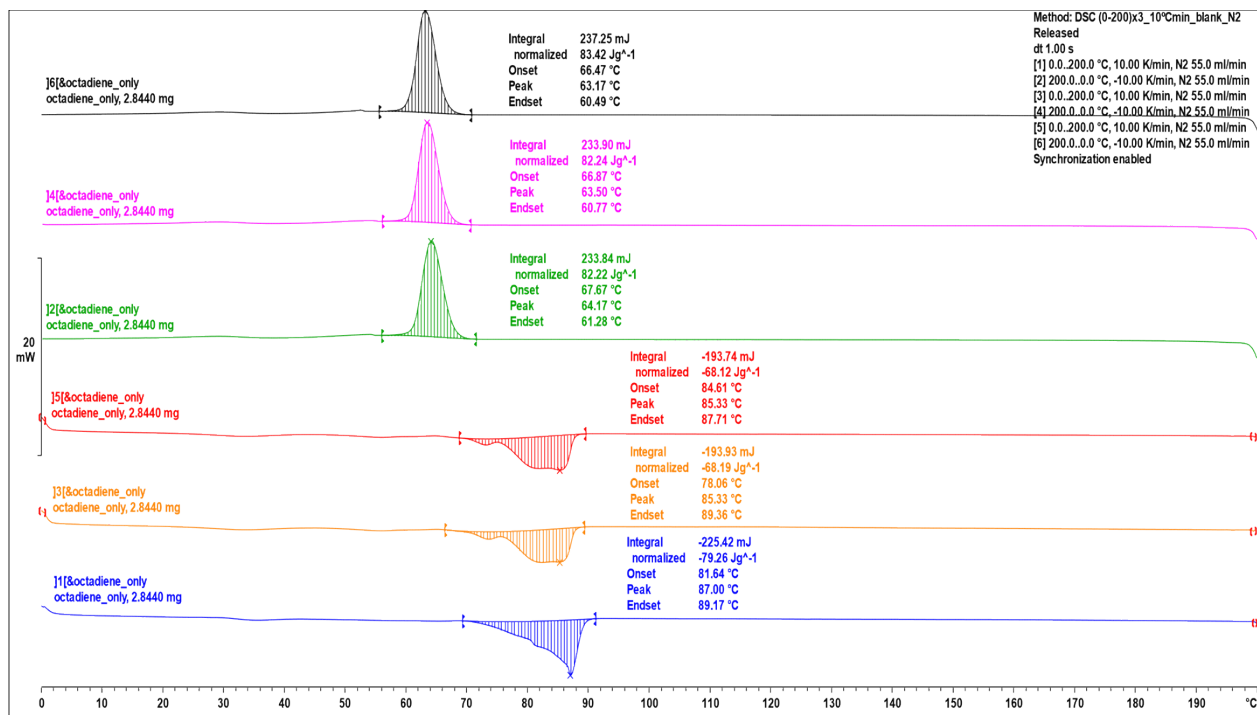
S25. DSC Analyses

Figure S21: DSC trace of M1

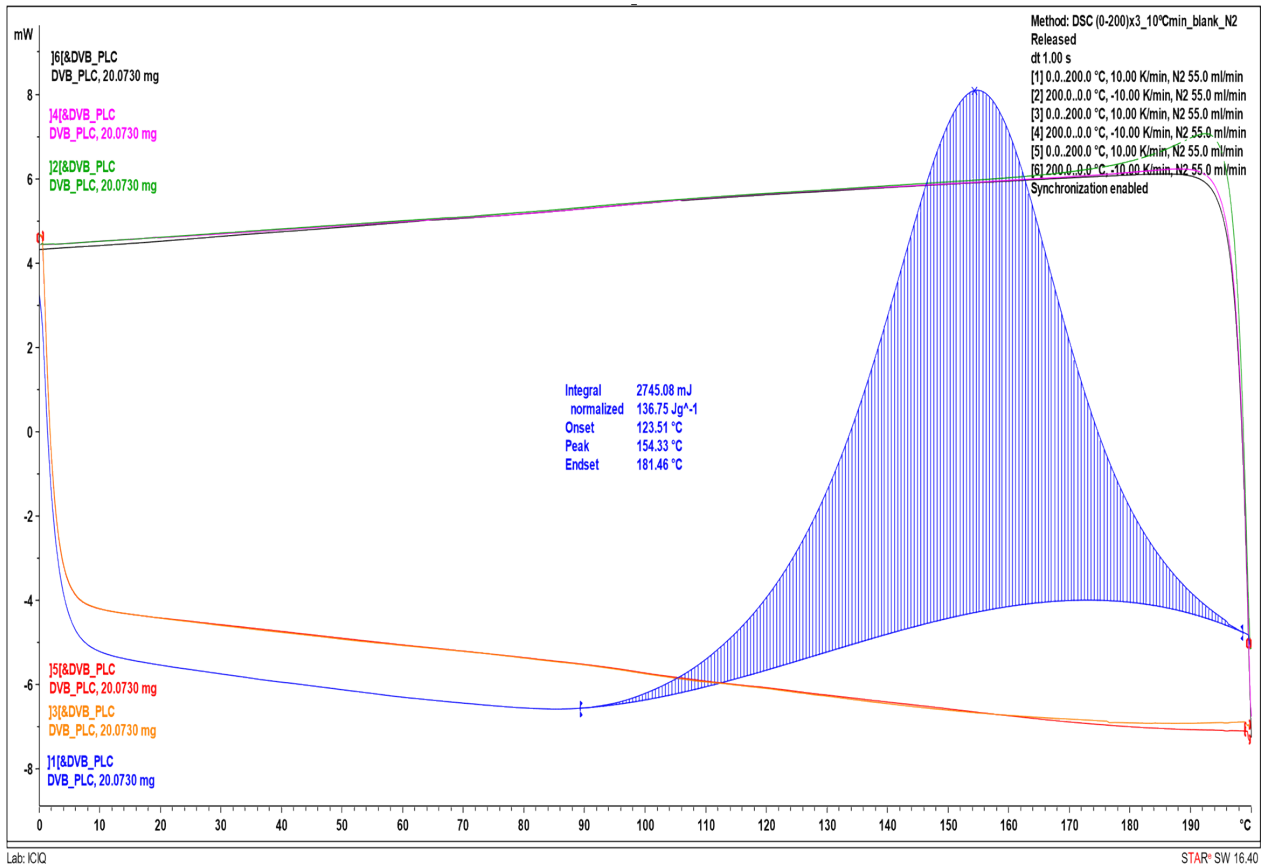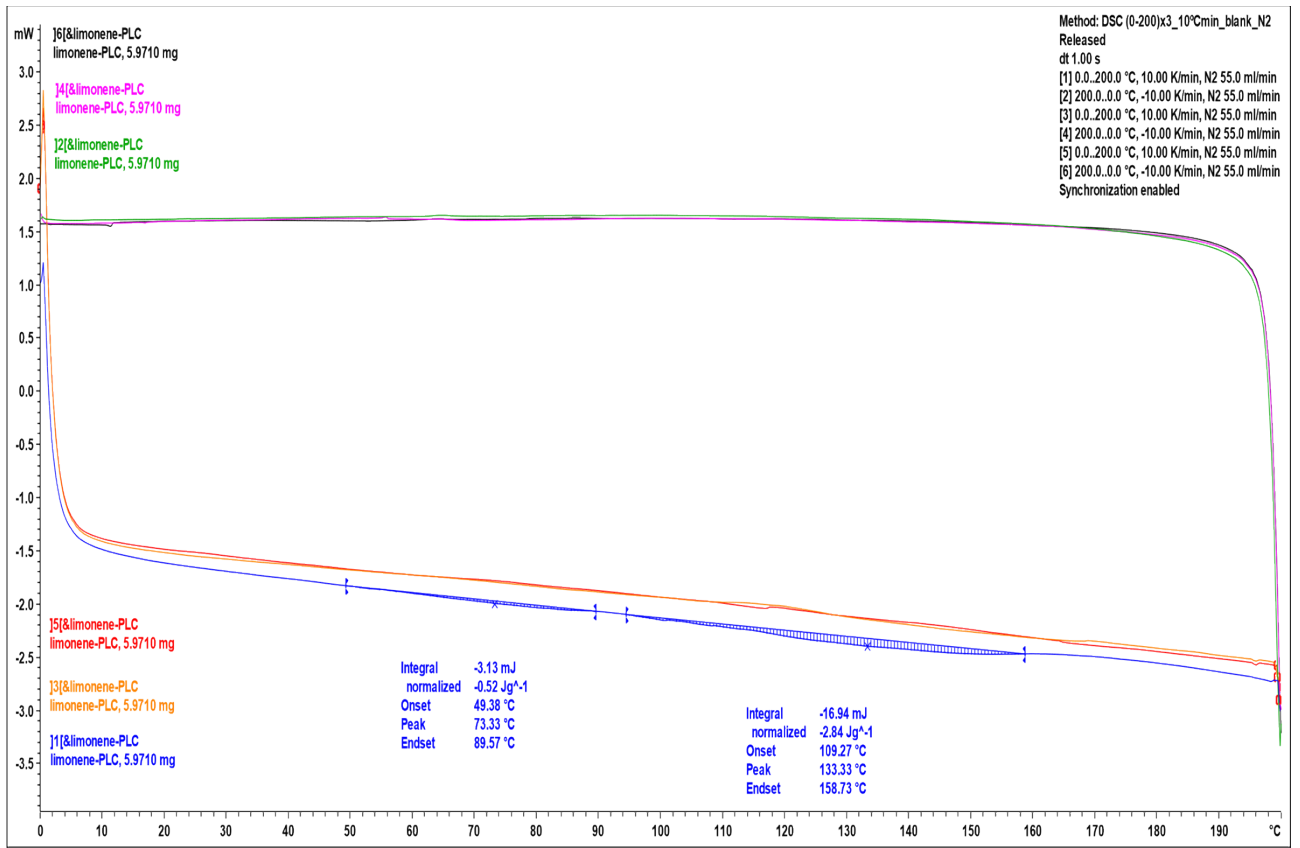*Figure S22: DSC trace of **M2***

*Figure S23: DSC trace of **M3***

*Figure S24: DSC trace of **M5**.*

S29. Results of Bending Test Analyses

Table S2: Analysis of bending test of cross-linked DVB (M1).			
SAMPLE	stress at break (MPa)	strain at break (%)	Bending Modulus (MPa)
Sample 1	0.219949	5.77656	4.5818
Sample 2	0.731029	5.53515	12.8290
Average	**0.475489**	**5.655855**	**8.7054**
Deviation	**0.361388134**	**0.170702648**	**5.831651046**

This sample was very difficult to test because it was very fragile and disintegrated when manipulating.

Table S3: Analysis of bending test of DVB-PLC (M3).			
SAMPLE	stress at break (MPa)	strain at break (%)	Bending Modulus (MPa)
Sample 1	1.24828	4.52689	35.9676
Sample 2	0.924718	4.2963	33.3639
Sample 3	0.888029	4.32908	28.9654
Average	**1.020342333**	**4.38409**	**32.76563333**
Deviation	**0.198250361**	**0.124749798**	**3.539229219**

S30. Results of Tensile Test Analyses

| Table S4: Tensile test analysis of Limonene-PLC M5.				
SAMPLE	stress at break (MPa)	strain at break (%)	Tensile Modulus (MPa)	Energy absorbed at break (KJ/m³)
Sample 1	0.1075338	33.32055	0.3500	20.23
Sample 2	0.1258417	35.09459	0.4000	23.44
Sample 3	0.1012498	34.41553	0.3200	18.22
Sample 4	0.1052566	29.0009	0.4100	19.57
Average	**0.109970475**	**32.9578925**	**0.37**	**20.36304748**
Deviation	**0.010895014**	**2.737364511**	**0.042426407**	**2.213455472**

S31. Photos of preparation samples
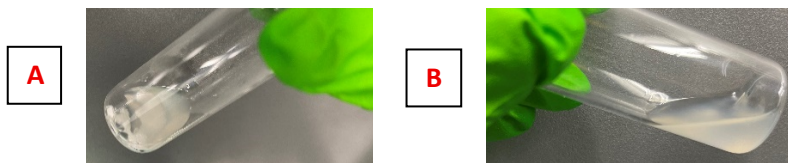
Figure S25: A) Heterogeneous mixture of PLC in DVB matrix at 30 wt% of PLC. B) Homogeneous mixture of PLC in DVB matrix at 20 wt% of PLC.

Figure S26: Heterogeneous mixture of PLC in 1,7-octadiene matrix at 30 wt% of PLC.

Figure S27: Heterogeneous mixture of PLC in limonene matrix at 30 wt% of PLC.

Figure S28: Heterogeneous mixture of PLC in geraniol matrix at 30 wt% of PLC.

Figure S29: Shape of material M3.
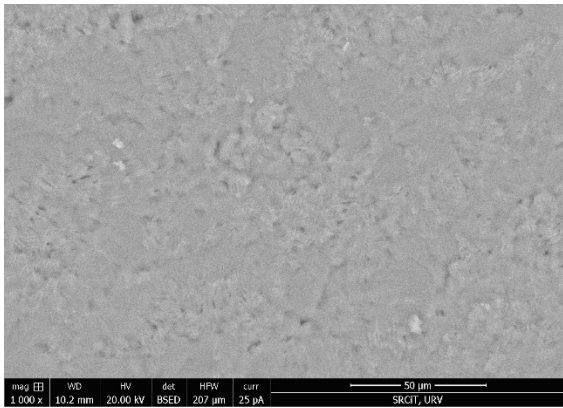
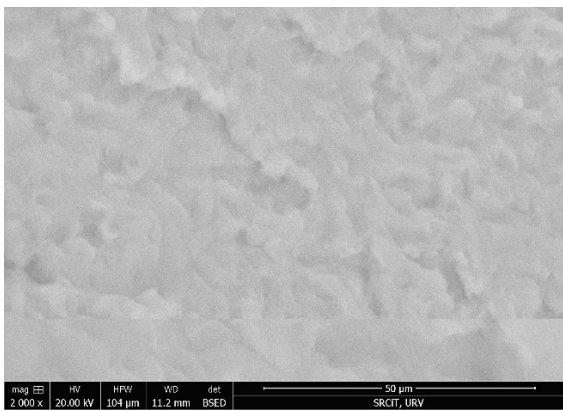## S32. SEM photos

Figure S30: SEM photo of material M2.
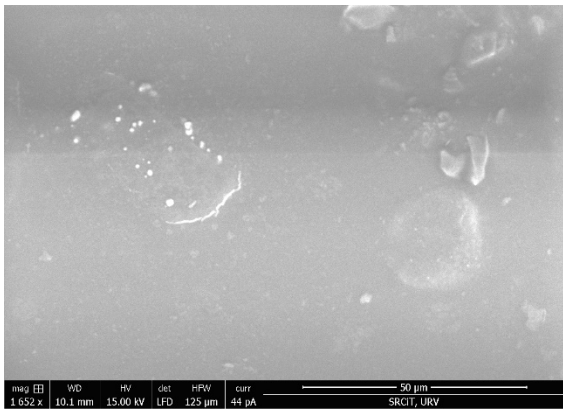

Figure S31: SEM photo of material M4.

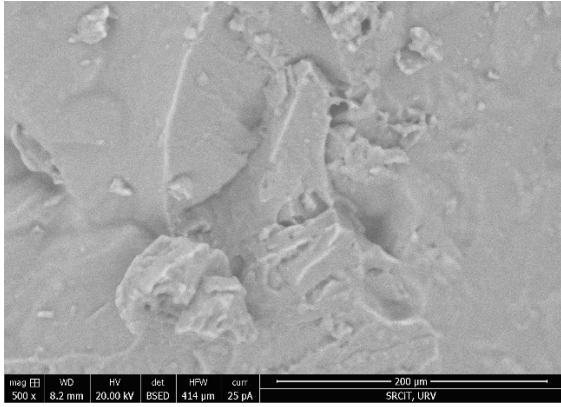*Figure S32: SEM photo of material M5.*

Figure S33: SEM photo of material M6.

S33. Molecular weight between crosslinks

The thermomechanical results from the DMA analyses allowed to derive the molecular weight between crosslinks[2]. The formula to obtain M_c (in g·mol^{-1}) is the following:

$$Mc = \frac{3 \cdot R \cdot Trubbery \cdot d}{E'rubbery}$$

R is the gas constant (8.3144626 m^3·Pa·K^{-1}·mol^{-1})

d is the skeletal density (g·m^{-3})

$T_{rubbery}$ (K) is the temperature at the rubbery state

$E'_{rubbery}$ (Pa) is the storage modulus derived from the DMA measured at the rubbery state.

To ensure that the measurement is within the plateau zone at the rubbery state, the $T_{rubbery}$ was taken 30°C above the Tg for PLC-crosslinked samples (M3-M6).

Table S5: Values of $T_{rubbery}$, $E'_{rubbery}$ and d (skeletal density) used to derive the molecular weight between crosslinkings (Mc) for PLC-crosslinked samples (M3-M6).

M	$T_{rubbery}$ (K)[a]	$E'_{rubbery}$ (MPa)[b]	skeletal density (g·cm^{-3})[c]	Mc (g·mol^{-1})[d]
M3	377,29	156.649	1.0733 ± 0.0017	64
M4	360,02	1.867	1.0783 ± 0.0017	5184
M5	301,32	26.055	1.1006 ± 0.0008	317
M6	274,51	0.044	1.1222 ± 0.0021	173220

[a] $T_{rubbery}$ when the samples are in the rubbery plateau.

[b] Value of the storage modulus deduced from the DMA experiment at the $T_{rubbery}$.

[c] Skeletal density measured at 22 °C in a gas pycnometer, using He as inert gas; the value is the average of 3 measurements; the ranges provided indicate a confidence level of 95%.

[d] Molecular weight between crosslinks.

S34. References

1. L. Peña Carrodeguas, J. González-Fabra, F. Castro-Gómez, C. Bo and A. W. Kleij, Al[III]-Catalysed Formation of Poly(limonene)carbonate: DFT Analysis of the Origin of Stereoregularity. *Chem. Eur. J.,* 2015**, 21**, 6115-6122.
2. I. M. Barszczewska-Rybarek, A. Korytkowska-Walach, M. Kurcok, G. Chladek and J. Kasperski, *Acta Bioeng. Biomech.*, 2017, **19**, 47-53.